

Integrating carbon–halogen bond formation into medicinal plant metabolism

Weerawat Runguphan^{1*}, Xudong Qu^{1†*} & Sarah E. O'Connor¹

Halogenation, which was once considered a rare occurrence in nature, has now been observed in many natural product biosynthetic pathways¹. However, only a small fraction of halogenated compounds have been isolated from terrestrial plants². Given the impact that halogenation can have on the biological activity of natural products¹, we reasoned that the introduction of halides into medicinal plant metabolism would provide the opportunity to rationally bioengineer a broad variety of novel plant products with altered, and perhaps improved, pharmacological properties. Here we report that chlorination biosynthetic machinery from soil bacteria can be successfully introduced into the medicinal plant *Catharanthus roseus* (Madagascar periwinkle). These prokaryotic halogenases function within the context of the plant cell to generate chlorinated tryptophan, which is then shuttled into monoterpene indole alkaloid metabolism to yield chlorinated alkaloids. A new functional group—a halide—is thereby introduced into the complex metabolism of

C. roseus, and is incorporated in a predictable and regioselective manner onto the plant alkaloid products. Medicinal plants, despite their genetic and developmental complexity, therefore seem to be a viable platform for synthetic biology efforts.

Numerous halogenase enzymes from soil bacteria have been identified and characterized extensively^{1,3–5}. Two of these flavoenzymes, PyrH^{6,7} and RebH^{8–11}, chlorinate the indole ring of tryptophan in the five and seven positions, respectively. Transferring these enzymes into other natural product pathways would allow site-specific incorporation of halogens onto a range of tryptophan-derived alkaloid products¹², provided that the downstream enzymes could accommodate the chlorinated tryptophan precursor.

Catharanthus roseus produces a wide variety of monoterpene indole alkaloids¹³ (Fig. 1a). This metabolic pathway begins with the conversion of tryptophan (1) to tryptamine (2) by tryptophan decarboxylase¹⁴. Tryptamine then condenses with the iridoid terpene

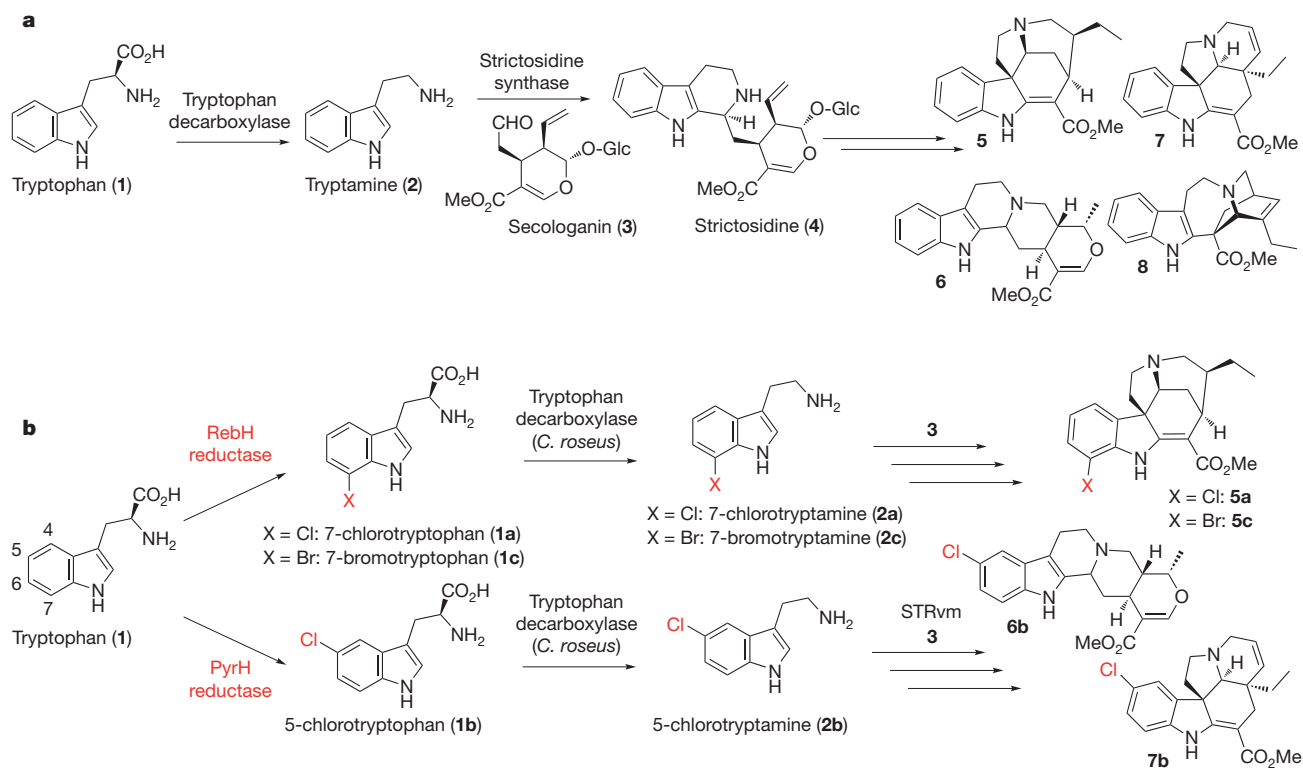


Figure 1 | Monoterpene indole alkaloid biosynthesis. **a**, Tryptophan (1) is decarboxylated by tryptophan decarboxylase to yield tryptamine (2), which reacts with secologanin (3) to form strictosidine (4). After numerous rearrangements, strictosidine (4) is converted into a variety of monoterpene indole alkaloids, such as 19,20-dihydroakuammicine (5), ajmalicine (6), tabersonine (7) and catharanthine (8). These compounds have a variety of

pharmacological activities^{24–26,30}. Me, CH₃; Glc, glucose. **b**, RebH and PyrH, along with a partner reductase, halogenate the indole ring of tryptophan to yield chlorotryptophan. Here we show that after transformation of these enzymes into *C. roseus*, the halogenated tryptophans **1a** and **1b** can be decarboxylated by tryptophan decarboxylase (*C. roseus*) to form the chlorotryptamines **2a** and **2b** and then converted into chlorinated monoterpene indole alkaloids.

¹Department of Chemistry, Massachusetts Institute of Technology, Cambridge, Massachusetts 02139, USA. [†]Present address: State Key Laboratory of Bioorganic and Natural Products Chemistry, Shanghai Institute of Organic Chemistry, Chinese Academy of Sciences, 345 Lingling Road, Shanghai 200032, China.

*These authors contributed equally to this work.

secologanin (**3**) to form a biosynthetic intermediate strictosidine (**4**), which is subsequently functionalized in *C. roseus* to form over 100 alkaloids, including the anticancer agent vinblastine¹³. Previous work has shown that when *C. roseus* cell culture is supplemented with a variety of halogenated tryptamines, the corresponding halogenated alkaloid analogues are produced in isolable yields^{15,16}. If prokaryotic halogenases could function in the eukaryotic plant cell, and if tryptophan decarboxylase could convert halogenated tryptophan into halogenated tryptamine, then *C. roseus* would produce chlorinated alkaloids *de novo* (Fig. 1b).

Because RebH and PyrH do not turn over tryptamine, this strategy requires that tryptophan decarboxylase from *C. roseus* recognize halogenated tryptophan. We assayed tryptophan decarboxylase from *C. roseus* *in vitro* with tryptophan ($K_m = 51.7 \pm 9.2 \mu\text{M}$ (Michaelis constant), $k_{\text{cat}} = 5.1 \pm 0.1 \text{ min}^{-1}$ (turnover number), $k_{\text{cat}}/K_m =$

$0.099 \mu\text{M}^{-1} \text{ min}^{-1}$), 7-chlorotryptophan (**1a**; $K_m = 499 \pm 74 \mu\text{M}$, $k_{\text{cat}} = 1.6 \pm 0.04 \text{ min}^{-1}$, $k_{\text{cat}}/K_m = 0.00327 \mu\text{M}^{-1} \text{ min}^{-1}$) and 5-chlorotryptophan (**1b**; $K_m = 538 \pm 48 \mu\text{M}$, $k_{\text{cat}} = 2.5 \pm 0.08 \text{ min}^{-1}$, $k_{\text{cat}}/K_m = 0.00455 \mu\text{M}^{-1} \text{ min}^{-1}$) (Supplementary Figs 1 and 2). The activity of the enzyme suggested that halogenated tryptophan could be decarboxylated *in vivo*.

When considering how to merge the prokaryotic biosynthetic machinery with the plant alkaloid pathway, we chose to transfer the halogenase enzymes into *C. roseus* rather than move the plant biosynthetic enzymes into a microbial host. Most of the monoterpene indole alkaloid biosynthetic genes have not been identified, making heterologous expression of this pathway impossible at present. Moreover, we note that reconstitution of plant alkaloid pathways continues to be a challenge^{17,18}. Many alkaloids use complex starting materials (such as secologanin) that are only produced by a few specialized plants, so

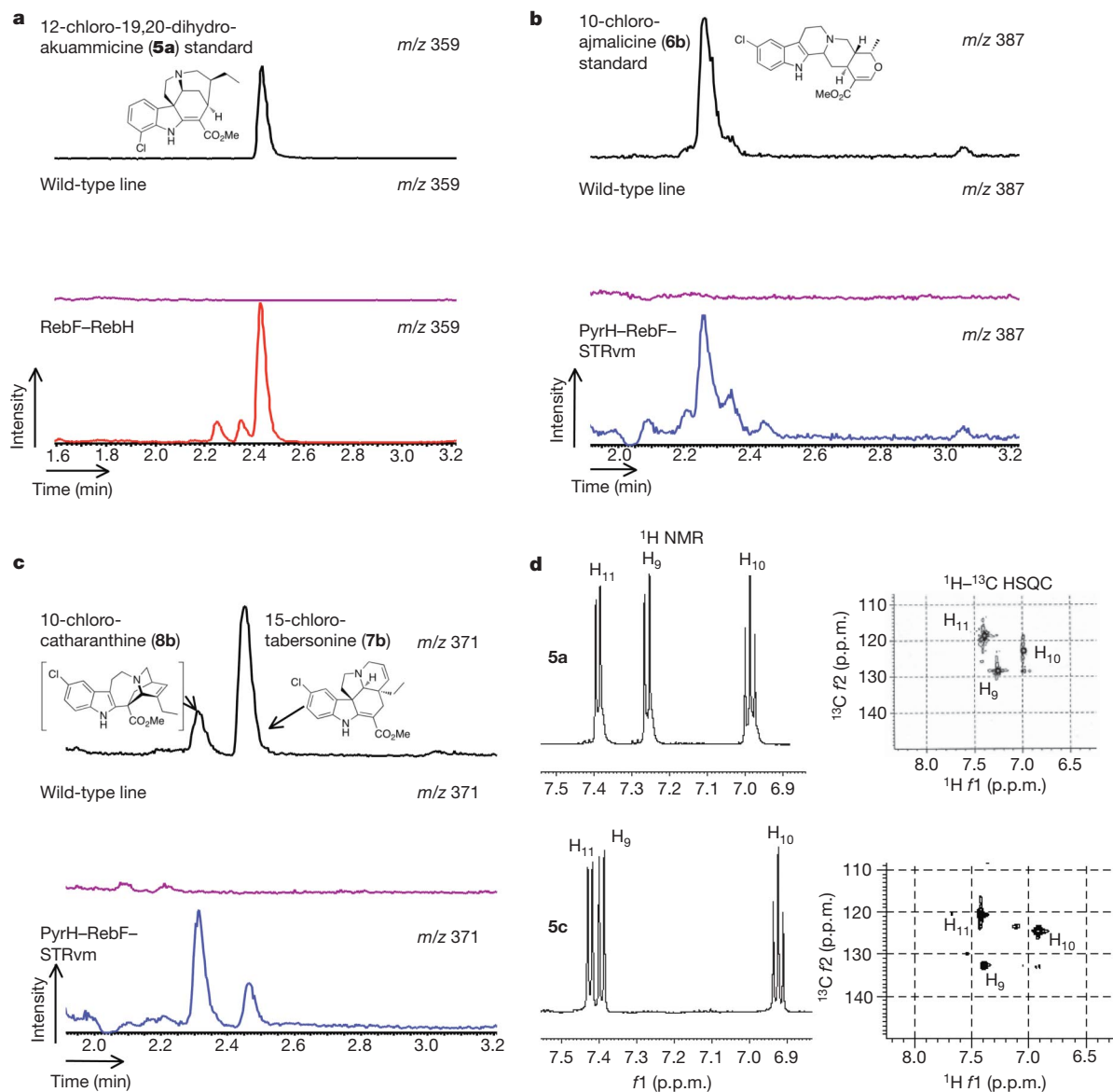


Figure 2 | Chlorinated alkaloids in *C. roseus* hairy root culture. **a**, LC-MS chromatograms showing 12-chloro-19,20-dihydroakuammicine (**5a**; m/z 359) in RebF-RebH hairy roots (red trace), contrasted with control cultures transformed with no plasmid (purple trace). An authentic standard of **5a** validated the structural assignment (black trace; Supplementary Figs 30 and 31). **b**, Chromatograms showing 10-chloroajmalicine (**6b**) in RebF-PyrH-STRvm hairy roots (blue trace), contrasted with control cultures (purple trace). An authentic standard of **6b** is shown²² (black trace). **c**, Chromatograms

showing 15-chlorotabersonine (**7b**) in RebF-PyrH-STRvm hairy roots (blue trace), contrasted with control cultures (purple trace). The other major peak at m/z 371 had an exact mass and ultraviolet spectrum consistent with a chlorinated analogue of catharanthine²² (**8**) (Supplementary Fig. 29). **d**, ^1H NMR and ^1H - ^{13}C heteronuclear single quantum coherence (HSQC) spectra of **5a** and **5c**. f_1 and f_2 , chemical shifts in the ^1H and ^{13}C dimensions, respectively.

reconstitution of plant alkaloid pathways must also include biosynthesis of these precursors. For example, ajmalicine (**6**; Fig. 1a), one of the simplest of the monoterpene indole alkaloids, requires an estimated 14 discrete enzymes for biosynthesis from tryptophan and the terpene geraniol¹³; reconstitution of a pathway of this length is a significant engineering problem. Therefore, we believe that exploring approaches in the host plant is an important aspect of alkaloid metabolic engineering efforts.

To produce 7-chlorotryptophan *in planta*, we generated an expression construct containing codon-optimized complementary DNA encoding the 7-tryptophan chlorinase RebH and its required partner flavin reductase, RebF, in a plant expression vector (pCambia1300), both under the control of constitutive cauliflower mosaic virus (CaMV) 35S promoters. For production of 5-chlorotryptophan, an expression construct encoding the 5-chlorinating enzyme PyrH, along with RebF as the partner reductase, was generated. No signal sequence was added to the halogenase genes, to ensure that RebH, PyrH and RebF would produce chlorinated tryptophan in the cytosol, where it would most readily encounter the decarboxylase, which is also localized in the cytosol¹⁹ (Supplementary Figs 3–5).

We used *Agrobacterium rhizogenes* to generate hairy root culture of *C. roseus* transformed with the halogenase genes²⁰. One of the early biosynthetic enzymes, strictosidine synthase, cannot turn over 5-chlorotryptamine²¹ (**2b**). Therefore, when transforming *C. roseus* with *pyrH* and *rebF*, we also introduced a mutant of strictosidine synthase (STRvm) that can convert 5-chlorotryptamine to 10-chlorostrictosidine^{16,22} (**4b**). After a selection process, we cultivated the transformed root culture on standard Gamborg's B5 plant medium and monitored chlorinated alkaloids using liquid chromatography/mass spectrometry (LC–MS). We observed formation of chlorinated tryptophans **1a** and **1b** and chlorinated alkaloids in both the RebH–RebF and PyrH–RebF–STRvm hairy root lines (Fig. 2 and Supplementary Figs 6–15). These results indicate that RebH, PyrH and the partner reductase function productively in the plant cell environment, demonstrating that the flavin halogenases are highly transportable among kingdoms. Because chlorinated alkaloid production was observed in the transformed lines, we conclude that tryptophan decarboxylase can competently turn over halogenated tryptophan substrates *in vivo*.

Hairy roots transformed with RebH and RebF, which produce 7-chlorotryptophan, yielded a major chlorinated product at *m/z* 359 (Fig. 2a). An authentic standard of 12-chloro-19,20-dihydroakuammicine (**5a**) co-eluted with this compound. Natural products containing the akuammicine scaffold have a variety of pharmacological activities^{23–25}. Although the parent compound, 19,20-dihydroakuammicine (**5**) has been isolated in good yields from other plants²⁶, it is not a major alkaloid in *C. roseus* hairy root culture. However, when wild-type *C. roseus* cell lines were incubated with 7-chlorotryptamine, 12-chloro-19,20-dihydroakuammicine was also the major chlorinated product (Supplementary Fig. 16). Therefore, the predominance of 12-chloro-19,20-dihydroakuammicine in the RebH–RebF hairy root line is probably due to substrate specificity of downstream enzymes for 7-chlorotryptamine. A hairy root line transformed with the 5-chlorotryptophan enzyme system, PyrH, RebF and STRvm, produced a variety of chlorinated alkaloids (Fig. 2b–d). Two representative chlorinated alkaloids, 10-chloroajmalicine (**6b**) and 15-chlorotabersonine (**7b**), were identified by co-elution with authentic standards²¹.

Chlorinated alkaloid production seemed to be stable over the course of at least six subcultures. The alkaloid 12-chloro-19,20-dihydroakuammicine was produced at 26 ± 4 μg per gram of fresh root weight of a representative cell line averaged over six subcultures. For comparison, wild-type cell lines produced ~ 25 μg per gram of fresh tissue weight of chlorinated alkaloids when the medium was supplemented with 200 μM 7-chlorotryptamine (**2a**). Similarly, 10-chloroajmalicine and 15-chlorotabersonine (**7b**) were produced at 2.8 ± 0.9 and 4.0 ± 1.0 μg per gram of fresh root weight, respectively, for a representative cell line averaged over four subcultures (Supplementary Figs

12 and 14). Different concentrations of KCl (3 μM –20 mM) were added to the medium, but increasing amounts of exogenous chloride salt did not significantly affect the yields of chlorinated alkaloids (Supplementary Figs 17 and 18).

Previous reports demonstrated that RebH can use bromide to yield brominated tryptophan⁸ (**1c**). To assess the capacity of RebH for bromination *in vivo*, we supplemented a low-chloride cell culture medium with KBr. The *in vitro* halide specificity of RebH correlated with the products generated *in vivo*, as we observed the formation of a compound that co-eluted with an authentic standard of 12-bromo-19,20-dihydroakuammicine (**5c**) (21 ± 8 and 49 ± 20 μg per gram of fresh root weight with 10 mM and 20 mM KBr supplementation, respectively; Fig. 3). In contrast, supplementation of the medium with KI failed to yield either iodinated tryptophan or iodinated alkaloids. Again, this correlated with *in vitro* studies showing that RebH does not accept iodide as a substrate⁸ (Supplementary Figs 19–22).

We also measured the transcript levels of the heterologous enzymes by real-time PCR with reverse transcription. The production of halogenated compounds depended on the expression of both RebF and RebH or PyrH. Notably, when the strictosidine synthase mutant STRvm was not expressed in the PyrH–RebF hairy root lines, we observed accumulation of 5-chlorotryptophan (representative cell line, 9 ± 1 μg per gram of fresh root weight) and 5-chlorotryptamine (representative cell line, 20 ± 9 μg per gram of fresh root weight), but did not observe downstream alkaloids (Supplementary Figs 23 and 24).

Tryptophan does not seem to accumulate in either wild-type or transformed hairy roots. However, accumulation of 7-chlorotryptophan (50 ± 12 μg per gram of fresh root weight for a representative RebH–RebF cell line) and 5-chlorotryptophan (8 ± 2 μg per gram of fresh root weight for a representative PyrH–RebF–STRvm cell line) was observed, suggesting that decarboxylation of chlorinated tryptophan is a bottleneck *in vivo*, a step that could potentially be subjected to future engineering efforts. This is consistent with the 30-fold-lower catalytic efficiency of the decarboxylase enzyme for halogenated

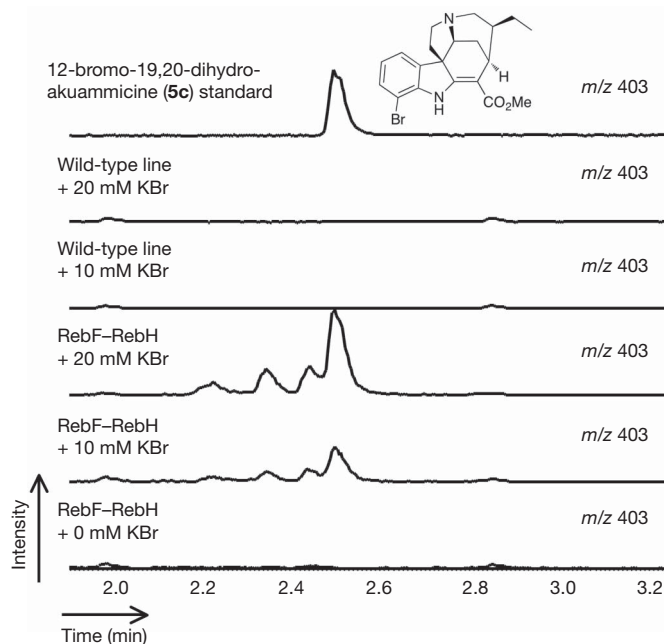


Figure 3 | Extracted LC–MS chromatograms showing the presence of 12-bromo-19,20-dihydroakuammicine (**5c**; *m/z* 403) in RebF–RebH hairy roots. Hairy roots are grown in medium supplemented with KBr (0–20 mM final concentration) for two weeks before alkaloid extractions. 12-bromo-19,20-dihydroakuammicine is not observed in control cultures transformed with no plasmid after incubation in KBr-supplemented medium. An authentic standard of 12-bromo-19,20-dihydroakuammicine is used to validate the structural assignment (Supplementary Figs 29, 30 and 32).

tryptophan *in vitro*. The morphologies of the halogen producing lines were thicker and slower growing than those of wild-type lines (Supplementary Fig. 25). Because tryptophan serves as the precursor for other small-molecule metabolites, we speculate that chlorinated tryptophan may be diverted into other pathways such as auxins. Notably, 4-chloro indole acetic acid, which is found in several species of pea, has altered activity relative to the auxin indole acetic acid^{27,28}.

Medicinal plants produce a wide range of complex natural products but generate relatively few halogenated compounds; chlorinated or brominated compounds are not found among the approximately 3,000 known monoterpene indole alkaloids produced by plants in the Apocynaceae, Rubiaceae and Loganiaceae families. The halogenation of natural products often has profound effects on the bioactivity of the compound, and can serve as a useful handle for further chemical derivatization^{1,29}. Despite the metabolic and developmental complexity of plant tissue, transformation of these prokaryotic genes led to the regioselective incorporation of halides into the alkaloid products of the existing plant pathway. Notably, the yield of chlorinated alkaloids in the most productive lines (~26 µg per gram of fresh weight of plant tissue) is only 15-fold lower than the yield of total natural alkaloids (compounds 5, 6, 7 and 8) from wild-type tissue (~420 µg per gram of fresh weight of plant tissue) (Supplementary Fig. 26). The ease with which we engineered the successful production of chlorinated alkaloids in *C. roseus*, a plant with limited genetic characterization, indicates that medicinal plants can provide a viable platform for synthetic biology.

METHODS SUMMARY

Structural characterization is shown in Supplementary Figs 27–32 and Supplementary Tables 1 and 2.

Generation of transgenic *C. roseus* hairy root cultures. We transformed the expression construct pCAMRebHRebF into *A. rhizogenes* ATCC 15834 by electroporation (1-mm cuvette, 1.25 kV), and we co-transformed pCAMPyrHRebF and pCAMSTRvm into *A. rhizogenes* ATCC 15834 by electroporation. Transformation of *C. roseus* seedlings with the generated *Agrobacterium* strains was performed as previously reported²⁰.

Evaluation of alkaloid production in transgenic *C. roseus* hairy roots. Every transgenic hairy root line that survived hygromycin selection medium was evaluated for alkaloid production. Transformed hairy roots were grown in Gamborg's B5 solid medium (half-strength basal salts, full-strength vitamins, 30 g l⁻¹ sucrose, 6 g l⁻¹ agar, pH 5.7). The total chloride concentration in Gamborg's B5 formulation was ~1 mM. We ground three-week-old hairy roots with a mortar, pestle and 106-µm acid-washed glass beads in methanol (10 ml g⁻¹ fresh weight of hairy roots). The crude natural product mixtures were filtered through 0.2-mm cellulose acetate membrane (VWR) and subsequently subjected to LC-MS analysis. Hairy roots transformed with wild-type *A. rhizogenes* lacking the plasmid were also evaluated.

Brominated alkaloid production in transgenic *C. roseus* hairy roots. We grew a selected transformed hairy root line for two weeks in low-chloride solid medium (67 mg l⁻¹ (NH₄)₂SO₄, 353 mg l⁻¹ Ca(NO₃)₂·4H₂O, 61 mg l⁻¹ MgSO₄, 1,250 mg l⁻¹ KNO₃, half-strength Murashige and Skoog micronutrient salts and full-strength Murashige and Skoog vitamins, 3 µM total chloride concentration). Hairy roots were transferred to the same medium supplemented with either potassium bromide or potassium iodide (10–20 mM final concentration) and cultivated for an additional two weeks. They were then processed and alkaloid production was analysed as described above (Supplementary Figs 12–15). We performed experiments in duplicate.

Full Methods and any associated references are available in the online version of the paper at www.nature.com/nature.

Received 26 April; accepted 20 September 2010.

Published online 3 November 2010.

1. Neumann, C. S., Fujimori, D. G. & Walsh, C. T. Halogenation strategies in natural products biosynthesis. *Chem. Biol.* **15**, 99–109 (2008).
2. Gribble, G. W. The diversity of naturally produced organohalogenes. *Chemosphere* **52**, 289–297 (2003).
3. Vaillancourt, F. H., Yeh, E., Vosburg, D. A., Garneau-Tsodova, S. & Walsh, C. T. Nature's inventory of halogenation catalysts: oxidative strategies predominate. *Chem. Rev.* **106**, 3364–3378 (2006).

4. van Pée, K. H. & Patallo, E. P. Flavin-dependent halogenases involved in secondary metabolism in bacteria. *Appl. Microbiol. Biotechnol.* **70**, 631–641 (2006).
5. Blasiak, L. C. & Drennan, C. L. Structural perspective on enzymatic halogenation. *Acc. Chem. Res.* **42**, 147–155 (2009).
6. Zehner, S. *et al.* A regioselective tryptophan 5-halogenase is involved in pyrroindomycin biosynthesis in *Streptomyces rugosporus* LL-42D005. *Chem. Biol.* **12**, 445–452 (2005).
7. Zhu, X. *et al.* Structural insights into regioselectivity in the enzymatic chlorination of tryptophan. *J. Mol. Biol.* **391**, 74–85 (2009).
8. Yeh, E., Garneau, S. & Walsh, C. T. Robust *in vitro* activity of RebF and RebH, a two-component reductase/halogenase, generating 7-chlorotryptophan during rebeccamycin biosynthesis. *Proc. Natl Acad. Sci. USA* **102**, 3960–3965 (2005).
9. Yeh, E. *et al.* Flavin redox chemistry precedes substrate chlorination during the reaction of the flavin-dependent halogenase RebH. *Biochemistry* **45**, 7904–7912 (2006).
10. Yeh, E., Blasiak, L. C., Koglin, A., Drennan, C. L. & Walsh, C. T. Chlorination by a long-lived intermediate in the mechanism of flavin-dependent halogenases. *Biochemistry* **46**, 1284–1292 (2007).
11. Bitto, E. *et al.* The structure of flavin-dependent tryptophan 7-halogenase RebH. *Proteins* **70**, 289–293 (2008).
12. Sánchez, C. *et al.* Combinatorial biosynthesis of antitumor indolocarbazole compounds. *Proc. Natl Acad. Sci. USA* **102**, 461–466 (2005).
13. O'Connor, S. E. & Maresh, J. Chemistry and biology of terpene indole alkaloid biosynthesis. *Nat. Prod. Rep.* **23**, 532–547 (2006).
14. De Luca, V., Marineau, C. & Brisson, N. Molecular cloning and analysis of cDNA encoding a plant tryptophan decarboxylase: comparison with animal dopa decarboxylases. *Proc. Natl Acad. Sci. USA* **86**, 2582–2586 (1989).
15. McCoy, E. & O'Connor, S. E. Directed biosynthesis of alkaloid analogs in the medicinal plant *Catharanthus roseus*. *J. Am. Chem. Soc.* **128**, 14276–14277 (2006).
16. Bernhardt, P., McCoy, E. & O'Connor, S. E. Rapid identification of enzyme variants for reengineered alkaloid biosynthesis in periwinkle. *Chem. Biol.* **14**, 888–897 (2007).
17. Hawkins, K. M. & Smolke, C. D. Production of benzyloquinoline alkaloids in *Saccharomyces cerevisiae*. *Nature Chem. Biol.* **4**, 564–573 (2008).
18. Minami, H. *et al.* Microbial production of plant benzyloquinoline alkaloids. *Proc. Natl Acad. Sci. USA* **105**, 7393–7398 (2008).
19. De Luca, V. & Cutler, A. J. Subcellular localization of enzymes involved in indole alkaloid biosynthesis in *Catharanthus roseus*. *Plant Physiol.* **85**, 1099–1102 (1987).
20. Hughes, E. H., Hong, S.-B., Shanks, J. V., San, K.-Y. & Gibson, S. I. Characterization of an inducible promoter system in *Catharanthus roseus* hairy roots. *Biotechnol. Prog.* **18**, 1183–1186 (2002).
21. Rungphan, W. & O'Connor, S. E. Metabolic reprogramming of periwinkle plant culture. *Nature Chem. Biol.* **5**, 151–153 (2009).
22. Loris, E. A. *et al.* Structure-based engineering of stricotosidine synthase: auxiliary for alkaloid libraries. *Chem. Biol.* **14**, 979–985 (2007).
23. Menzies, J. R., Paterson, S. J., Duwiejua, M. & Corbett, A. D. Opioid activity of alkaloids extracted from *Picralima nitida* (fam. Apocynaceae). *Eur. J. Pharmacol.* **350**, 101–108 (1998).
24. Frédéricich, M. *et al.* Antiplasmodial activity of alkaloids from various strychnos species. *J. Nat. Prod.* **65**, 1381–1386 (2002).
25. Zhu, W.-M. *et al.* Components of stem barks of *Winchia calophylla* A. DC. and their bronchodilator activities. *J. Integr. Plant Biol.* **47**, 892–896 (2005).
26. Amat, M., Linares, A. & Bosch, J. A new synthetic entry to pentacyclic Strychnos alkaloids. Total synthesis of (+-)-tubifolidine, (+-)-tubifoline, and (+-)-19,20-dihydroakuammicine. *J. Org. Chem.* **55**, 6299–6312 (1990).
27. Gandar, J. C. & Nitsch, C. Isolement de l'ester méthylique d'un acide chloro-3-indolyllactique à partir de graines immatures de pois, *Pisum sativum* L. *C. R. Acad. Sci. (Paris) Ser. D* **265**, 1795–1798 (1967).
28. Marumo, S., Hattori, H., Abe, H. & Munakata, K. Isolation of 4-chloroindolyl-3-acetic acid from immature seeds of *Pisum sativum*. *Nature* **219**, 959–960 (1968).
29. Deb Roy, A., Gruschow, S., Cairns, N. & Goss, R. J. Gene expression enabling synthetic diversification of natural products: chemogenetic generation of pacidamycin analogs. *J. Am. Chem. Soc.* **132**, 12243–12245 (2010).
30. Li, S. *et al.* Assessment of the therapeutic activity of a combination of almitrine and raubasine on functional rehabilitation following ischaemic stroke. *Curr. Med. Res. Opin.* **20**, 409–415 (2004).

Supplementary Information is linked to the online version of the paper at www.nature.com/nature.

Acknowledgements We acknowledge support from the NIH (GM074820) and the American Cancer Society (RSG-07-025-01-CDD). We thank H.-Y. Lee and M. Tjandra for assistance with NMR characterizations and L. Li for high-resolution mass spectroscopy analysis.

Author Contributions All authors contributed to experimental design and data analysis. X.Q. initiated the project and its design, and performed steady-state kinetics. W.R. developed and implemented the transformation strategy and performed steady-state kinetics and metabolite analysis. All authors contributed to the preparation of the manuscript.

Author Information Reprints and permissions information is available at www.nature.com/reprints. The authors declare no competing financial interests. Readers are welcome to comment on the online version of this article at www.nature.com/nature. Correspondence and requests for materials should be addressed to S.E.O.C. (soc@mit.edu).

METHODS

Heterologous expression and purification of *C. roseus* tryptophan decarboxylase. The tryptophan decarboxylase (TDC) gene (accession number M25151.1) was obtained by reverse-transcription PCR (RT-PCR) amplification of mRNA isolated from *C. roseus* hairy root culture (Invitrogen, Dynabeads mRNA direct kit) with PCR primers that introduce sites for NdeI and XhoI (underlined): 5'-AAAAACATATGGGCAGCATTGATCAACA-3' and 5'-AAAAAACTCGAGTCAAGCTTCTTGAGCAAATC-3'. The PCR fragment was subcloned into the pGEM-T Easy Vector (Promega), and then excised and ligated into the NdeI/XhoI site of the pET28-a plasmid (Novagen). The resulting pET28a-TDC construct was subsequently transformed into BL21 (DE3) pLysS electrocompetent *Escherichia coli* (Promega). A single *E. coli* colony harbouring pET28a-TDC was inoculated in 5 ml lysogeny broth medium supplemented with kanamycin (0.05 mg l⁻¹) and incubated overnight at 37 °C with shaking at 225 r.p.m. An aliquot of the overnight culture (1 ml) was then used to inoculate 100 ml lysogeny broth medium supplemented with kanamycin (0.05 mg l⁻¹) and incubated at 37 °C with shaking at 225 r.p.m. until OD₆₀₀ 0.6 was reached. Cells were induced for overexpression by the addition of isopropyl-β-D-galactopyranoside (IPTG; final concentration, 1 mM) and the culture was allowed to continue growth for 16 h at 18 °C. Cells were harvested by centrifugation and lysed by sonication. The hexahistidine-tagged TDC was purified using Ni-NTA Spin Kit (Qiagen) using manufacturer's protocols (Supplementary Fig. 1). Eluted enzyme was subsequently buffer-exchanged into phosphate buffer (50 mM NaH₂PO₄, 100 mM NaCl, pH 8.0) and immediately assayed for activity. This enzyme was not stable after extended storage.

Determining the steady-state kinetic constants of TDC for tryptophan substrate analogues, 5- and 7-chlorotryptophan (1b and 1a). Steady-state kinetic constants of TDC for 5- and 7-chlorotryptophan (1b and 1a) (Amatek) were determined in phosphate buffer (0.1 M NaH₂PO₄, 3.5 mM β-mercaptoethanol, pH 8.5) containing 1 mM pyridoxal-5'-phosphate at 30 °C (0.3-ml reaction volume) with TDC concentrations appropriate for obtaining the initial rate of the reaction (0.6–0.9 μM). Aliquots (25 μl) were quenched in 1 ml methanol, containing yohimbine (500 nM) as an internal standard, at appropriate time points. The samples were centrifuged (13,000 r.p.m. (16,000g), 5 min) to remove particulates and then analysed by LC-MS. Samples were ionized by ESI with a Micromass LCT Premier TOF Mass Spectrometer. The liquid chromatography was performed on an Acquity Ultra Performance BEH C18, 1.7 μm, 2.1 × 100 mm column on a gradient of 10–90% acetonitrile/water (0.1% formic acid) over 5 min at a flow rate of 0.6 ml min⁻¹. The appearance of the corresponding tryptamine analogues (either 5- or 7-chlorotryptamine) was monitored by peak integration and normalized to the internal standard. 5-chlorotryptamine was obtained from a commercial source (Alfa Aesar). 7-chlorotryptamine was synthesized as previously reported³. Eight substrate concentrations (200–2,500 μM) were tested for 7-chlorotryptophan substrate, and six substrate concentrations (200–1,200 μM) were tested for 5-chlorotryptophan substrate. Each concentration was assayed three times and the average values are reported with standard deviations. The data were fitted using nonlinear regression to the Michaelis–Menten equation using ORIGINPRO 7 (OriginLab). For reference, the kinetic constants for the natural substrate tryptophan (1) were also measured at concentrations ranging from 15 to 350 μM (Supplementary Fig. 2).

Construction of halogenase plant expression vectors PyrH–RebF–STRvm and RebH–RebF. The construction of plant expression vectors is summarized below and in Supplementary Fig. 3.

(i) The CaMV35S:Gus:NosPolyA fragment was obtained by PCR amplification of pCAMBIA1305.1 (Cambia) with forward and reverse PCR primers CaMV35S-NosPolyA that introduce sites for XbaI and KpnI at the 5' end, and PstI and SpeI at the 3' end (underlined): 5'-ACTTCTAGAGGTACCGGATCCTCTAGAGTCCGACCTGCAG-3' and 5'-ATTCTGCAGACTAGTCCCGATCTAGTAACATAGATGACACCG-3'.

(ii) The tryptophan 5-halogenase gene (*pyrH*; accession number AAU95674) was obtained by PCR amplification of genomic DNA isolated from *Streptomyces rugosporus* NRRL 21084 with forward and reverse PCR primers CrPyrH that introduce sites for XhoI and NcoI at the 5' end, and SpeI and BstEII at the 3' end (underlined): 5'-ACTCTCGAGCCATGGATATCCGATCTGTGGTATCG-3' and 5'-ACTACTAGTGGTAACCTCATTGGATGCTGGCGAGGTA-3'.

(iii) The flavin reductase gene (*rebF*; accession number BAC15756) was obtained by PCR amplification of genomic DNA isolated from *Lechevalieria aerocolonigenes* ATCC 39243 with forward and reverse PCR primers CrRebF that introduce sites for XhoI and NcoI at the 5' end, and SpeI and PmlI at the 3' end (underlined): 5'-ACTCTCGAGCCATGGATACGATCGAGTTCGACAGAC-3' and 5'-ACTACTAGTACAGTGTATCCCTCCGGTGTCCACAC-3'.

(iv) The tryptophan 7-halogenase gene (*rebH*; accession number BAC15758) was obtained by PCR amplification of genomic DNA isolated from *Lechevalieria*

aerocolonigenes ATCC 39243 with forward and reverse PCR primers CrRebH that introduce sites for SpeI and NcoI at the 5' end, and SpeI and PmlI at the 3' end (underlined): 5'-AAGACTACTAGTCCATGGATTCGGCAAGATTGAC-3' and 5'-ACTACTAGTACAGTGTACGCGCCGTGCTGTTGCC-3'.

CaMV35S:Gus:NosPolyA, PyrH, RebH and RebF PCR fragments were individually ligated into pGEM-Teasy vector (Promega) to yield pGEMCaMV35S, pGEMPyrH, pGEMRebH and pGEMRebF, respectively.

(v) Codon-optimization for *C. roseus* was performed to ensure efficient expression of the prokaryotic halogenase and flavin reductase genes in plant cell culture. Using codon usage database software (<http://www.kazusa.or.jp/codon/>), the following codons were identified as occurring at low frequency (triplet, frequency per thousand): GCG, 4.8; CGG, 3.3; ACG, 4.0; TCG, 6.1; CCG, 6.0; and CCC, 6.7. Site-directed mutagenesis was performed using a Stratagene QuikChange Site-Directed Mutagenesis kit to replace rare codons with the most frequently occurring codons encoding the corresponding amino acids. Only codons that appeared within the first 300 nucleotides of the genes were subjected to mutagenesis.

The site-directed-mutagenesis primers (name, sequence) were as follows (the sites of mutation are underlined): PyrH-SDM-for1, 5'-GTGGTGGTGGC ACTGCTGGCTGGATGACC-3'; PyrH-SDM-rev1, 5'-GGTCATCCAGCCAGC AGTGCCACCACCCAC-3'; PyrH-SDM-for2, 5'-GACATGCGGCCGTACAC TACTGCTACCCGATGAGCGCCGGC-3'; PyrH-SDM-rev2, 5'-GCCGGCG CTCATCGCGGTAGCAGTAGTGTACGCCGATGC-3'; RebH-SDM-for, 5'-CCCCAATCTGCAGACTGCTTCTTCGACTTCCTCGGA-3'; RebH-SDM-rev, 5'-TCCGAGGAAGTCAAGAAAGCAGTCTGCAGATTGGGG-3'; RebF-SDM-for1, 5'-ACCGCGCGGATCACA AGGGCTCTGATGAGCCTGTTCC-3'; RebF-SDM-rev1, 5'-GGGAAACAGGGCTCATCAGAGCCCTGTGATCGGCC CGGGT-3'; RebF-SDM-for2, 5'-CTCGTCTGCCTGAAC AGGGCTAGCGGAA CGTTGCAC-3'; RebF-SDM-rev2, 5'-GTGCAACGTTCCCGCT AGCCCTGTTC AGGCAGACGAG-3'.

(vi) pGEMCaMV35S was digested and ligated into the KpnI/EcoRI sites of pSP72 vector (Promega) to yield pSPCaMV35S.

(vii) pGEMRebH and pGEMRebF were digested and ligated into the NcoI/PmlI sites of pSPCaMV35S to yield pSPRebH and pSPRebF, respectively. Similarly, pGEMPyrH was digested and ligated into the NcoI/BstEII sites of pSPCaMV35S to yield pSPPyRH. pSPRebF was then digested and ligated into the PstI site of pSP72 to yield pSPRebF-2.

(viii) pSPRebH and pSPPyRH were digested and ligated into the XbaI/EcoRI sites of pSPRebF-2 to yield pSPRebHRebF and pSPPyRHRebF, respectively. Finally, both pSPRebHRebF and pSPPyRHRebF were digested and ligated into the SpeI site of pCAMBIA1300A to yield pCAMRebHRebF and pCAMPyrHRebF. pCAMBIA1300A was constructed by introducing an SpeI restriction into pCAMBIA1300 (Cambia). The site-directed-mutagenesis primers are (SpeI site underlined) 5'-CCCCTTCAGTTAAACTAGT CAGTGTTCGACAGGAT-3' and 5'-atcctgtaaacactg ACTAGT ttaactgaagcggg-3'.

pCAMSTRvm was constructed as previously described²¹.

Generation of transgenic *C. roseus* hairy root cultures. The plant expression construct pCAMRebHRebF was transformed into *A. rhizogenes* ATCC 15834 by means of electroporation (1-mm cuvette, 1.25 kV). pCAMPyrHRebF and pCAMSTRvm were co-transformed into *A. rhizogenes* ATCC 15834 via electroporation (1mm cuvette, 1.25 kV). Transformation of *C. roseus* seedlings with the generated *Agrobacterium* strains was performed as previously reported²¹. Briefly, 180–250 *C. roseus* seedlings (Vinca Little Bright Eyes, Nature Hills Nursery) were germinated aseptically on Gamborg's B5 medium (full-strength basal salts, full-strength vitamins, 30 g l⁻¹ sucrose, pH 5.7) and grown in a 16-h light, 8-h dark cycle at 26 °C for 3 weeks. Seedlings were then wounded with extra-fine forceps at the stem tip, and 3–5 μl *A. rhizogenes* from a freshly grown liquid culture were inoculated on the wound.

Hairy roots appeared at the wound site 2–3 weeks after infection for about 80% of the seedlings infected. After hairy roots reached 1–4 cm in length (usually about 6 weeks after infection), they were excised and transferred to Gamborg's B5 solid medium (half-strength basal salts, full-strength vitamins, 30 g l⁻¹ sucrose, 6 g l⁻¹ agar, pH 5.7) containing hygromycin (0.03 mg ml⁻¹) for selection and the antibiotic cefotaxime (0.25 mg ml⁻¹) to remove remaining bacteria. The total chloride concentration in Gamborg's B5 formulation was 1 mM. All cultures were grown in the dark at 26 °C. After the hygromycin selection process, hairy roots were maintained in solid medium lacking both hygromycin and cefotaxime.

To adapt the line to liquid culture, approximately 200 mg of hairy roots (typically five 3–4-cm-long stem tips) from each line that grew successfully on solid medium were transferred to 50 ml of half-strength Gamborg's B5 liquid medium. The cultures were grown at 26 °C in the dark at 125 r.p.m. Hairy root growth in liquid medium seemed to be slower than that in solid medium. Hairy root transformants were screened for survival in solid medium supplemented with hygromycin. The number of transformants decreased significantly after solid medium

selection for each of the constructs transformed. Every line that grew in the selection medium was analysed for alkaloid production.

Hairy root selection and adaptation processes. For the plasmid pCAMRebH/RebF, the number of transformed hairy roots was 200 and the number of hairy roots after solid medium selection was 31. For the plasmid pCAMPyrH/RebF/STRvm, the number of transformed hairy roots was 140 and the number of hairy roots after solid medium selection was 57.

Verification of transferred DNA integration by genomic DNA analysis. To verify the integration of transferred DNA (T-DNA) into the plant genome, the genomic DNA from transformed hairy roots was isolated (Qiagen DNeasy kit) and then subjected to PCR amplification using T-DNA-specific primers with TDC primers serving as a positive control (see below). Specifically, for the pCAMRebH/RebF hairy roots, primers for PCR amplification were designed to amplify the complete TDC gene (TDC_for and TDC_rev), a 660-base-pair (bp) region of the RebH gene (RebH_for and RebH_rev), a 680-bp region of the RebF gene (RebF_for and RebF_rev) and an 800-bp region of the selection marker HPT gene (HPT_for and HPT_rev) (see below).

PCR primers for verification of T-DNA integration of transformed hairy roots were as follows (name, sequence): TDC_for, 5'-AAAAAACAATATGGGCAGCATTGATCAACA-3'; TDC_rev, 5'-AAAAAACTCGAGTCAAGCTTCTTTGAGCAAATC-3'; RebH_for, 5'-GTCTTCGATGCCGACCTCTTC-3'; RebH_rev, 5'-GTACATGTCGATCTTCTCCTGC-3'; RebF_for, 5'-TAGAGGACCTAACAGAAC-3'; RebF_rev, 5'-CGTGACACTGGTCAGGGA-3'; HPT_for, 5'-GCCTGAACTCACCGCGACGTC-3'; HPT_rev, 5'-CCTCCAGAAGAAGATGTTGGC-3'.

PCR amplification of genomic DNA from all of the selected transformed lines (pCAMRebH/RebF cell line 4, lanes 1–4; pCAMRebH/RebF cell line 5, lanes 5–8; pCAMRebH/RebF cell line 6, lanes 9–12; pCAMRebH/RebF cell line 10, lanes 13–16; and pCAMRebH/RebF cell line 11, lanes 17–20) was successful for all four sets of primers (Supplementary Fig. 4). PCR amplification of hairy root transformed with *A. rhizogenes* lacking the pCambia vector (provided by Professor Jacqueline Shanks (Iowa State University) and Professor Carolyn Lee-Parsons (Northeastern University)) genomic DNA was successful only when TDC-specific primers were used (lanes 21–24). These results indicated that *rebH* and *rebF* were successfully incorporated into the *C. roseus* genome in all chosen lines.

For the pCAMPyrH/RebF/STRvm hairy roots, primers for PCR amplification were designed to amplify the complete TDC gene (TDC_for and TDC_rev), the complete PyrH gene (PyrH_for and PyrH_rev), a 680-bp region of the RebF gene (RebF_for and RebF_rev), a 440-bp region of the STRvm gene and an 800-bp region of the selection marker HPT gene (HPT_for and HPT_rev) (see below and Supplementary Fig. 5).

PCR primers for verification of T-DNA integration of transformed hairy roots were as follows (name, sequence): TDC_for, 5'-AAAAAACAATATGGGCAGCATTGATCAACA-3'; TDC_rev, 5'-AAAAAACTCGAGTCAAGCTTCTTGTAGCAAATC-3'; PyrH_for, 5'-ATGATCCGATCTGTGGTG-3'; PyrH_rev, 5'-TCATTGGATGCTGGCGAG-3'; RebF_for, 5'-TAGAGGACCTAACAGAAC-3'; RebF_rev, 5'-CGTGACACTGGTCAGGGA-3'; STRvm_for, 5'-CCTTATTATTGAAAGAGCTACATATG-3'; STRvm_rev, 5'-GCTAGAAACATAAGAAATTTCCCTTG-3'; HPT_for, 5'-GCCTGAACTCACCGCGACGTC-3'; HPT_rev, 5'-CCTCCAGAAGAAGATGTTGGC-3'.

PCR amplification of genomic DNA from three of four of the selected transformed lines (pCAMPyrH/RebF/STRvm cell line 1, lanes 1–5; pCAMPyrH/RebF/STRvm cell line 3, lanes 6–10; pCAMPyrH/RebF/STRvm cell line 6, lanes 11–15) was successful for all five sets of primers (Supplementary Fig. 5). PCR amplification of genomic DNA from pCAMPyrH/RebF/STRvm cell line 7 (lanes 16–20) was successful when TDC, PyrH, RebF and HPT primers were used but not when STRvm primers were used. PCR amplification of hairy root transformed with *A. rhizogenes* lacking the pCambia vector genomic DNA was successful only when TDC specific primers were used (lanes 21–25).

Evaluation of alkaloid production in transgenic *C. roseus* hairy roots. Every transgenic hairy root line that survived hygromycin selection medium was evaluated for alkaloid production. Transformed hairy roots were grown in Gamborg's B5 solid medium (half-strength basal salts, full-strength vitamins, 30 g l⁻¹ sucrose, 6 g l⁻¹ agar, pH 5.7). The total chloride concentration in Gamborg's B5 formulation was ~1 mM. Three-week-old hairy roots were ground with a mortar, pestle and 106 µm acid-washed glass beads in methanol (10 ml g⁻¹ of fresh hairy root weight). The crude natural product mixtures were filtered through 0.2-µm cellulose acetate membrane (VWR) and subsequently subjected to LC–MS analysis. Additionally, hairy roots transformed with wild-type *A. rhizogenes* lacking the plasmid were also evaluated.

These crude alkaloid mixtures were diluted 30:830 with methanol for mass spectral analysis. Samples were ionized by ESI with a Micromass LCT Premier TOF Mass Spectrometer. The liquid chromatography was performed on an Acquity Ultra Performance BEH C18, 1.7 µm, 2.1 × 100 mm column on a gradient

of 10–90% acetonitrile/water (0.1% TFA) over 5 min at a flow rate of 0.6 ml min⁻¹. The capillary and sample cone voltages were 1,300 and 60 V, respectively. The desolvation and source temperature were 300 and 100 °C, respectively. The cone and desolvation gas flow rates were 60 and 800 l per hour, respectively. Analysis was performed with MASSLYNX 4.1. Accurate mass measurements were obtained in W-mode. The spectra were processed using the MASSLYNX 4.1 mass measure, in which the mass spectrum of peaks of interest was smoothed and centred with TOF mass correction, locking on the reference infusion of reserpine. Data for RebF–RebH lines are shown in extracted LC–MS chromatograms in Supplementary Figs 6–10.

Feeding of 7-chlorotryptamine (2a) in control *C. roseus* hairy root cultures transformed with no plasmid. Alkaloid accumulation levels in hairy roots transformed with RebH and RebF were compared with alkaloid accumulation levels in control hairy root fed with 7-chlorotryptamine. The control hairy root line was grown for 2 weeks in half-strength Gamborg's B5 solid medium. Hairy roots were then transferred to the same medium supplemented with 7-chlorotryptamine (2a; 0, 25, 50, 100, 200 and 750 µM final concentrations) and grown for a further 1 week. Hairy roots were then processed and alkaloid production analysed as described in the previous subsection (Supplementary Fig. 16). Feeding studies were performed in duplicate.

Brominated alkaloid production in transgenic *C. roseus* hairy roots. A selected transformed hairy root line was grown for 2 weeks in low-chloride solid medium (67 mg l⁻¹ (NH₄)₂SO₄, 353 mg l⁻¹ Ca(NO₃)₂·4H₂O, 61 mg l⁻¹ MgSO₄, 1,250 mg l⁻¹ KNO₃, half-strength Murashige and Skoog micronutrient salts and full-strength Murashige and Skoog vitamins, 3 µM total chloride concentration). Hairy roots were transferred to the same medium supplemented with either potassium bromide or potassium iodide (10–20 mM final concentration) and cultivated for an additional 2 weeks. Hairy roots were then processed and alkaloid production analysed as described in the previous subsection but one. Hairy roots transformed with wild-type *A. rhizogenes* lacking the plasmid were also evaluated (Supplementary Figs 19–22). Experiments were performed in duplicate.

Purification and isolation of alkaloids from transformed TDC suppressed hairy roots supplemented with 7-chlorotryptamine and 7-bromotryptamine. To obtain chlorinated and brominated alkaloid standards, root tips (10–15) from TDC suppressed hairy roots³² were subcultured in six 50 ml Gamborg's B5 liquid medium (half-strength basal salts, full-strength vitamins, 30 g l⁻¹ sucrose, pH 5.7) and grown at 26 °C in the dark at 125 r.p.m. for 3 weeks before the medium was supplemented with either 7-chlorotryptamine (2a) or 7-bromotryptamine (2c) (750 µM final concentration). Both tryptamine analogue substrates were synthesized as previously reported³³. After 2 weeks of co-cultivation, hairy roots were extracted as described above in methanol (10 ml g⁻¹ fresh hairy root weight). Alkaloid extracts were filtered, concentrated under vacuum and redissolved in 25% acetonitrile/water (0.1% TFA) (1 ml g⁻¹ of fresh hairy root weight).

For cultures supplemented with 7-chlorotryptamine (2a), the redissolved mixture was purified on a 10 × 20 mm Vydac reverse-phase column using a gradient of 25–52% acetonitrile/water (0.1% TFA) over 24 min. Alkaloids were monitored at 228 nm and fractions containing the alkaloid analogues of interest, as determined by the characteristic isotopic distribution expected for chlorinated molecules (³⁵Cl/³⁷Cl) from LC–MS analysis, were combined and concentrated under vacuum (Supplementary Fig. 27).

For cultures supplemented with 7-bromotryptamine (2c), similar procedures were performed to isolate alkaloids from transgenic hairy roots, except that the liquid chromatography method was extended to 26 min. Alkaloids were monitored at 228 nm and fractions containing the alkaloid analogues of interest, as determined by LC–MS analysis, were combined and concentrated under vacuum (Supplementary Fig. 28).

Isolated alkaloids from both feedings were analysed by LC–MS (same parameters as above), analytical high-performance liquid chromatography and, where possible, high resolution LC–MS (Supplementary Table 1), ultraviolet–visible spectroscopy (Supplementary Fig. 29), tandem MS–MS (Supplementary Fig. 30) and ¹H NMR, ¹³C NMR and ¹H–¹³C HSQC using a Bruker AVANCE-600 NMR spectrometer equipped with a 5-mm IH{13C,31P} cryoprobe (Supplementary Figs 31 and 32). Halogenated alkaloids generally displayed longer retention times than the natural alkaloids.

Quantification of chlorinated alkaloid production in transformed hairy roots. 12-chloro-19,20-dihydroakuammicine (5a) and 12-bromo-19,20-dihydroakuammicine (5c) standard curves were constructed by quantifying the peak areas of several concentrations (20–1,400 nM) of each alkaloid authentic standard using MASSLYNX 4.1. Similarly, 10-chloroajmalicine (6b), 15-chlorotabersonine (7b) and 10-chlorocatharanthine (8b) standard curves were constructed by quantifying the peak areas of several concentrations (20–1,400 nM) of each natural (that is, non-chlorinated) alkaloid authentic standard using MASSLYNX 4.1.

Dependence of chlorinated alkaloid production on concentrations of sodium chloride. A selected transformed hairy root line was grown for 2 weeks in low-chloride solid medium (67 mg l^{-1} $(\text{NH}_4)_2\text{SO}_4$, 353 mg l^{-1} $\text{Ca}(\text{NO}_3)_2 \cdot 4\text{H}_2\text{O}$, 61 mg l^{-1} MgSO_4 , $1,250 \text{ mg l}^{-1}$ KNO_3 , half-strength Murashige and Skoog micronutrient salts and full-strength Murashige and Skoog vitamins, $3 \mu\text{M}$ total chloride concentration). Hairy roots were transferred to the same medium supplemented with potassium chloride ($0\text{--}20 \text{ mM}$ final concentration) and grown for a further 2 weeks. Hairy roots were then processed and alkaloid production was analysed as previously described (Supplementary Figs 17 and 18).

Assessment of the stability of chlorinated alkaloid production in subsequent subcultures. Ten root tips from hairy roots transformed with pCAMRebH/RebF and pCAMPyrH/RebF/STRvm were subcultured every 3 weeks in Gamborg's B5 solid medium (half-strength basal salts, full-strength vitamins, 30 g l^{-1} sucrose, 6 g l^{-1} agar, pH 5.7), and grown at 26°C in the dark. Alkaloids were isolated from 21-day-old hairy roots and analysed as described above (Supplementary Figs 11–14).

Verification of expression of RebH, RebF and PyrH, STRvm enzymes by real-time RT-PCR. Real-time RT-PCR was used to assess the expression levels of RebH and RebF. Expression levels in hairy roots infected with *A. rhizogenes* lacking the pCAMRebH/RebF construct were compared with expression levels in hairy roots harbouring pCAMRebH/RebF. Messenger RNA from transformed hairy roots was isolated and purified from contaminant DNA using a Qiagen RNeasy Plant Mini Kit and Rnase-free DnaseI, respectively. The resulting mRNA was then reverse-transcribed to cDNA using a Qiagen QuantiTect Reverse transcription kit and then subjected to PCR with specific primers (see below), a Qiagen SYBR Green PCR kit and a Biorad DNA Engine Opticon 2 system. The threshold cycle (C_T) was determined as the cycle with a signal higher than that of the background plus 10 s.d. *Catharanthus roseus* 40S ribosomal protein S9 (Rps9), encoded by a house-keeping gene, was used to adjust the amount of the total mRNA in all samples. Real-time RT-PCR was performed in triplicate and the data are pictured as the relative expression levels of *rebH* and *rebF* mRNA in transgenic hairy roots as well as hairy roots lacking the pCAMBIA plasmid (Supplementary Fig. 23).

PCR primers for real-time RT-PCR of pCAMRebH/RebF transformed hairy roots were designed using the GenScript web tool (<http://www.genscript.com/ssl-bin/app/primer>), and were as follows (name, sequence): RebH_for, 5'-GACGG

GCATCTACTTCGTCT-3'; RebH_rev, 5'-TCGAACATCGTCTCGATCTC-3' (amplicon size, 117); RebF_for, 5'-CTGATGAGCCTGTTTCCCA-3'; RebF_rev, 5'-CGTGACACTGGTCAGGGA-3' (amplicon size, 99); Rbps9_for, 5'-TTGAGC CGTATCAGAAATGC-3'; Rbps9_rev, 5'-CCCTCATCAAGCAGACCATA-3' (amplicon size, 122).

Real time RT-PCR was used to assess the expression levels of PyrH, RebF and STRvm. Expression levels in hairy roots infected with *A. rhizogenes* lacking the pCAMPyrH/RebF/STRvm construct were compared with expression levels in hairy roots harbouring pCAMPyrH/RebF/STRvm (Supplementary Fig. 24).

Chlorinated alkaloid production in a line lacking STRvm expression is shown in Supplementary Fig. 15. Photographs of the transformed roots are shown in Supplementary Fig. 25.

PCR primers for real-time RT-PCR of pCAMPyrH/RebF/STRvm transformed hairy roots were designed using GenScript web tool, and were as follows (name, sequence): PyrH_for, 5'-GCCTGCTCATCAACCAGAC-3'; PyrH_rev, 5'-CATC GCGGTAGCAGTAGTGT-3' (amplicon size, 137); RebF_for, 5'-CTGATGAG CCTGTTTCCCA-3'; RebF_rev, 5'-CGTGACACTGGTCAGGGA-3' (amplicon size, 99); STRvm_for, 5'-TATTATTGAAAGACTACATATG-3'; STRvm_rev, 5'-CTCTGCACTGCCTTTCTTG-3' (amplicon size, 134); Rbps9_for, 5'-TTGA GCCGTATCAGAAATGC-3'; Rbps9_rev, 5'-CCCTCATCAAGCAGACCATA-3' (amplicon size, 122).

Quantification of natural alkaloids in wild-type roots. The levels of natural alkaloids in wild type hairy roots was quantified as described in section on quantification of chlorinated alkaloid production in transformed hairy roots.

The levels of the four most abundant alkaloids found in these hairy roots, ajmalicine (6), tabersonine (7), catharanthine (8), as well as tryptophan (1) and tryptamine (2), were measured (Supplementary Fig. 26).

31. Hughes, E. H. *et al.* Characterization of an inducible promoter system in *Catharanthus roseus* hairy roots. *Biotechnol. Prog.* **18**, 1183–1186 (2002).
32. Runguphan, W. *et al.* Silencing of tryptamine biosynthesis for production of nonnatural alkaloids in plant culture *Proc. Natl Acad. Sci. USA* **106**, 13673–13678 (2009).
33. Schumacher, R. W. *et al.* Synthesis of didemnomolines A-D, N9-substituted β -carboline alkaloids from the marine ascidian *Didemnum* sp. *Tetrahedron* **55**, 935–942 (1999).